HAL
open science

Thiazolidinediones Induce Osteocyte Apoptosis by a G Protein-coupled Receptor 40-dependent Mechanism

Aleksandra Mieczkowska, Michel-Félix Baslé, Daniel Chappard, Guillaume Mabilleau

To cite this version:

Aleksandra Mieczkowska, Michel-Félix Baslé, Daniel Chappard, Guillaume Mabilleau. Thiazolidinediones Induce Osteocyte Apoptosis by a G Protein-coupled Receptor 40-dependent Mechanism. Journal of Biological Chemistry, 2012, 287 (28), pp.23517 - 23526. 10.1074/jbc.M111.324814 . hal-03262120

HAL Id: hal-03262120

https://univ-angers.hal.science/hal-03262120v1

Submitted on 16 Jun 2021

HAL is a multi-disciplinary open access archive for the deposit and dissemination of scientific research documents, whether they are published or not. The documents may come from teaching and research institutions in France or abroad, or from public or private research centers.

L'archive ouverte pluridisciplinaire **HAL**, est destinée au dépôt et à la diffusion de documents scientifiques de niveau recherche, publiés ou non, émanant des établissements d'enseignement et de recherche français ou étrangers, des laboratoires publics ou privés.

THIAZOLIDINEDIONES INDUCED OSTEOCYTE APOPTOSIS BY A GPR40-DEPENDENT MECHANISM

Aleksandra Mieczkowska[1,2], Michel F. Baslé[2,3], Daniel Chappard[2] , Guillaume Mabilleau[1,2,3]

From Nuffield Department of Orthopaedics, Rheumatology and Musculoskeletal Sciences - University of Oxford, Oxford, United Kingdom[1], GEROM – LHEA [2] and Service Commun d'Imageries et d'Analyses Microscopiques[3], Institut de Biologie en Santé, LUNAM Université d'Angers, CHU d'Angers, 49933, Angers, France

Running title: Thiazolidinediones and osteocytes

Address correspondence to: Guillaume Mabilleau, PhD, GEROM-LHEA, Institut de Biologie en Santé – IRIS, LUNAM Université d'Angers, 49933 Angers Cedex 09, France. Phone: +33 244688349, Fax: +33 244688350, Email: guillaume.mabilleau@univ-angers.fr

Keywords: Thiazolidinedione, osteocyte, GPR40, sclerostin, apoptosis

Background: Thiazolidinediones mediate osteocyte apoptosis and sclerostin up-regulation with an unknown mechanism.
Results: Osteocyte apoptosis is mediated through activation of Erk 1/2 and p38 whilst sclerostin up-regulation is through PPAR-γ signaling.
Conclusion: TZDs signal not exclusively through PPAR-γ as thought but also via a surface receptor called GPR40.
Significance: Learning how TZDs signal into bone cells is crucial to prevent adverse effect associated with the use of these drugs.

SUMMARY

Thiazolidinediones represent an interesting treatment in type 2 diabetes mellitus. However adverse effects such as heart problems and bone fractures have already been reported. Previously, we reported that pioglitazone and rosiglitazone induce osteocyte apoptosis and sclerostin up-regulation; however, the molecular mechanisms leading to such effects are unknown. In this study, we found that thiazolidinediones rapidly activated Erk 1/2 and p38. These activations were mediated through ras proteins and GPR40, a receptor expressed at the surface of osteocytes. Activation of this pathway conducted only to osteocyte apoptosis but not sclerostin up-regulation. On the other hand, thiazolidinediones were capable of activating PPAR-γ, and activation of this signalling pathway led to sclerostin up-regulation but not osteocyte apoptosis. This study evidenced two distinct signalling pathways activated in osteocytes in response to thiazolidinediones that could participate to the observed increase in fractures in thiazolidinedione-treated patients.

Thiazolidinediones (TZDs), also known as glitazones, represent a class of pharmaceutical compounds approved for the treatment of type 2 diabetes mellitus. TZDs are PPARγ agonists and as such upon binding to PPARγ, TZDs promote target gene transcription and protein expression (1). Increased interest for TZDs has emerged with the results of a randomised trial called "A Diabetes Outcome Progression Trial" (ADOPT) demonstrating a durable effect on glycated haemoglobin as compared with sulphonylurea or metformin (2). However, adverse effects have been reported with TZDs use such as weight gain, fluid retention and increased risks of congestive heart failure (2,3). Also, an unexplained increased risk of bone fracture has been documented mostly in women but to date the causes are unknown (2-5). Several cell types coexist in bone, osteoblasts (the bone-forming cells), osteoclasts (bone-resorbing cells), osteocytes (which control bone remodelling) and bone marrow cells including adipocytes. Adipocytes and osteoblasts come from a common progenitor upon activation of specific transcription factors. Activation of Runx-2 drives progenitors to become osteoblasts whilst activation of PPAR-γ results in adipocyte differentiation. As TZDs are PPAR-γ agonists it has been postulated that TZDs increase adipocyte differentiation at the expense of osteoblasts in vitro (6,7). In vivo models showed that TZDs decrease bone formation and increase

adiposity in the bone marrow although bone resorption was not affected (8-12).

The effects of TZDs on osteocytes are poorly understood. In the adult skeleton, osteocytes make up more than 90-95% of all bone cells compared with 4-6% osteoblasts and 1-2% osteoclasts (13). These cells are regularly dispersed throughout the mineralised matrix, connected to each other and to cells on the bone surface through dendritic processes generally radiating toward the bone surface and the blood supply. Osteocytes are a target of drugs affecting bone metabolism such as bisphosphonates because of their connections with blood vessels (14,15). Osteocytes can conduct and control both bone resorption and bone formation by expressing key mediators such as RANKL and sclerostin (16). Recently, we reported that TZDs induce osteocyte apoptosis in a dose –dependent manner (17). Furthermore, we also evidenced that TZD-treated osteocytes up-regulated the expression of sclerostin, a bone formation inhibitor, whilst RANKL expression was unchanged as compared with untreated cells (17). However, the molecular pathways involved in such effects are totally unknown.

As TZDs are PPARγ agonists, they were thought to signal exclusively through this nuclear receptor. Several recent studies show that TZDs also activate a membrane G-protein coupled receptor called GPR40 (18,19). GPR40 is a fatty acid receptor activated by long-chain fatty acids. Furthermore, GPR40 is involved in glucose- and fatty acid-induced insulin secretion (20,21). However, the expression and role of GPR40 in bone is unknown.

The aim of this study was to investigate the signalling pathways involved in osteocytes apoptosis and sclerostin expression. We found that although TZDs induce sclerostin expression through a PPAR-γ mechanism, osteocyte apoptosis is mediated via GPR40 and activation of Erk 1/2 and p38.

Experimental procedures

Reagents- Rosiglitazone and troglitazone were purchased from Cayman Chemicals (Ann Arbor, MI). Pioglitazone was purchased from Molekula (Shaftesbury, UK). Signalling inhibitors were purchased from Calbiochem (Nottingham, UK). Alpha-MEM, foetal bovine serum (FBS), bovine calf serum, penicillin and streptomycin were purchased from Lonza (Wokingham, UK). Antibodies were purchased from Cell Signaling Technology (Danvers, MA) when otherwise stated. All other chemicals were purchased from Sigma-Aldrich (Poole, UK).

Animals- Calvariae (frontal and parietal bones) from 4 weeks old female Swiss mice were removed aseptically. The periosteal layers on both side were carefully stripped off with tweezers under α-MEM and calvariae were transferred into a collagen-coated T75 cm² flask prior to culture in αMEM supplemented with 5% FBS, 5% bovine calf serum, 100 U/mL penicillin, and 100 μg/mL streptomycin. At confluency, cells were detached with collagenase and plated as described below. This research was conducted in compliance with appropriate guidelines from the institutional animal care and use committee.

MLO-Y4 cells- The murine long bone–derived osteocytic cell line MLO-Y4 was kindly provided by L. Bonewald (University of Missouri-Kansas City, Kansas City, MO). These cells present features of osteocytes (16). Cells were cultured in αMEM supplemented with 5% FBS, 5% bovine calf serum, 100 U/mL penicillin, and 100 μg/mL streptomycin. Cells were plated at 1×10^4 cells/cm^2 on collagen type I–coated plates as described previously (22). Growth arresting was investigated in reducing FBS to 0.5% and bovine calf serum to 0.5%.

MTT assay-Cell proliferation was investigated using 3-(4,5dimethyl-thiazol-2yl)2,5-diphenyl tetrazolium bromide (MTT) as previously published (23).

Osteoclast cultures- Bone marrow macrophages from long bones of 4 weeks old female Swiss mice were harvested as previously described (24). Osteoclasts were generated using 25 ng/ml recombinant M-CSF (R&D Systems Europe, Abingdon, UK), 100 ng/ml recombinant soluble RANKL (Peprotech Ltd, London, UK) and 10^{-6}M thiazolidinediones. After 7 days of cultures, TRAP staining was performed as previously reported (25) and multinucleated cells with more than three nuclei were counted as osteoclasts.

Inhibition of intracellular signalling- in order to investigate specific signalling pathways, MLO-Y4 cells were cultured in the presence of the signalling inhibitors bisindoleimide I (50nM), farnesylthiosalicylic acid (20µM), FR180204 (10µM) or SB203580 (10µM) for 1h prior to addition of 10^{-6}M TZDs. These concentrations have been selected based on a previous pilot study. Sclerostin expression and cell apoptosis were investigated 24h later as described below.

Apoptosis assay- Apoptosis was determined in TZD-treated cultures as reported earlier (17). Briefly, after cell culture, the supernatant containing floating cells was collected and put in previously labelled eppendorf tubes. Each well was washed in PBS before trypsin was added to detach adherent cells. The mixture containing detached adherent cells was collected and pooled in the eppendorf containing the cell culture supernatant. Cells were spun at 1500 rpm for 10 minutes, the supernatant was removed carefully and cells were incubated with trypan blue 0.04% and transferred into a haemocytometer. Living (clear) and dead (blue) cells were counted under light microscope examination and the percentage of dead cells was determined for each condition as follow:

% of dead cells = 100 x (Number of dead cells) / (Number of dead cells + Number of living cells)

Western blot analysis/Immunoblotting- Cells were cultured in the presence of 10^{-6}M TZDs for the indicated period of time. Cells were washed in cold PBS and lysates were made by using a lysis buffer containing 50mM Tris-HCl pH 7.5, 100 mM NaCl, 50 mM NaF, 3 mM Na_3VO_4, protease inhibitor cocktail and 1% Nonidet P-40. Samples were spun at 13,000 rpm for 30 min at 4°C, the supernatant was collected and protein concentration was determined by BCA assay (ThermoScientific, Brebières, France). Samples (20µg per lane) were run on a 10% acrylamide gel and blotted onto a PVDF membrane. The membranes were washed in Tris buffered saline (TBS) and blocked with 5% bovine serum albumin. Samples were incubated overnight with one of the following specific antibodies for Erk1/2, phospho-Erk1/2 (Thr202/Tyr204), p38, phospho-p38 (Thr180/Tyr182- R&D Systems Europe, Abingdon, UK), sclerostin (R&D Systems Europe), PPAR-γ (SantaCruz Biotechnology, Heidelberg, Germany), phospho-PPAR-γ (Ser 84, SantaCruz Biotechnology), GPR40 (SantaCruz Biotechnology) and β-actin (Sigma-Aldrich). Subsequently membranes were washed in TBS and incubated with the appropriate secondary antibodies coupled to HRP (R&D Systems Europe). Immunoreactive bands were visualised using an ECL kit (Amersham, UK). The degree to which the different markers were induced was determined by normalizing the specific signal to that of β-actin using ImageJ Freeware (NIH). Control of loading was assessed by ponceau red staining of the membrane after transfer.

Silencing- SiGENOME SMARTpool siRNAs (containing a mixture of four siRNAs) targeting murine PPAR-γ sequences CGAAGAAC-CAUCCGAUUGA, ACCCAAUGGUUGCUG-AUUA, UCACAAUGCCAUCAGGUUU and CGACAUGAAUUCCUUAAUG and ON-TARGETplus SMARTpool siRNAs targeting murine GPR40 sequences GGAGAAAC-CUGUUGUGAUU, GGACAAAGUUGCUGA-AAUC, GUUCAUAGUUUGAGCGUUA and GAUAUGAUGUAGAGUUUGA; and non specific control siRNA duplexes were purchased from Thermo Fisher Scientific (Epsom, UK). Cells at a concentration of 5 x 10^3 cells/cm² were plated in either 6 wells plates or 25 cm² flasks coated with collagen type I as described above and cultured in the presence of 10^{-6}M TZDs. After 24h, cells were washed twice in Opti-MEM (Invitrogen) and preincubated with a mixture of 100 nM siRNA, oligofectamine (Invitrogen) and Opti-MEM. Cells were exposed to this transfection mixture for 16h before being returned to normal culture medium. Forty-eight hours after transfection, 10^{-6}M TZDs was added in the cultures. Knockdown efficiency was assessed by Western blotting.

Generation of reactive oxygen species- MLO-Y4 cells were plated at a density of 1 x 10^4 cells/cm² and cultured for up to 60 minutes in the presence of TZDs. At the end of the incubation period, intracellular levels of reactive oxygen species were determining using dichloro-fluorescein diacetate (DCFH-DA) as previously described (26) and fluorescence was read with a M2 microplate reader (Molecular Devices, Saint Grégoire, France) with an excitation wavelength of 488 nm and emission wavelength of 530 nm. As a positive control, MLO-Y4 cells were

incubated in the presence of 100 nM phorbol myristate acetate.

Transmitting electron microscopy- MLO-Y4 cells were fixed in paraformaldehyde 3.7% in Sorensen's buffer. Then cells were dehydrated in a graded series of ethanol and embedded in Lowicryl K4M. Ultrathin sections were cut and immunodetection of GPR40 and BAX (R&D Systems Europe) were done using a secondary antibody complexed with 10 nm-gold beads.

Statistical analysis-Statistical analysis was performed with the Systat® statistical software release 11.0 (Systat Inc. San José; CA). Results were expressed as mean ± standard error of the mean. The non-parametric Kruskall-Wallis test was used to compare the differences between the groups. When significant differences were observed, data were subjected to Mann-Whitney U test. Differences at $p < 0.05$ were considered significant. Experiments were repeated at least four times.

Results

The rapid activation of Erk1/2 and p38 is PPAR-γ independent- As represented Figure 1, within 15 minutes of incubation with TZDs, a rapid and massive phosphorylation of Erk1/2 and p38 could be noted in osteocytes. This activation lasted for up to 60 minutes. On the other hand, no phosphorylations of Akt or JNK were recorded in the presence of TZDs (data not shown). As these activations were rapid, we hypothesised that they did not require PPAR-γ. To test this hypothesis, we performed silencing of this nuclear receptor. Interestingly, after 15 minutes treatment with pioglitazone or rosiglitazone, although expression of PPAR-γ was reduced by 90 % after 72hours as compared to cells treated with scrambled siRNA, activations of Erk1/2 and p38 were unchanged. This seems to indicate that these two signalling pathways were activated independently of PPAR-γ. Several previous studies reported a role for TZDs in inducing oxidative stress in cells leading to activation of MAP Kinase independently of PPAR-γ. However, no increase in reactive oxygen species generation was recorded in the presence of TZDs (Fig 1C).

Activation of Erk1/2 and p38 is Ras-dependent - As PKC and Ras are two targets of TZDs in other tissues, we decided to investigate their role in Erk1/2 and p38 activation. The use of bisindoleimide I, a specific inhibitor of PKC, did not reduce the activation of Erk1/2 or p38 in response to pioglitazone or rosiglitazone (Figure 2A). On the other hand, the use of farnesylthiosalicylic acid, a specific inhibitor of Ras proteins hampered activation of Erk1/2 and p38 in pioglitazone- or rosiglitazone-treated cells (Figure 2B). These results suggest that activation of Erk1/2 and p38 is dependent of proteins from the Ras family.

Sclerostin up-regulation is PPAR-γ– dependent whilst MLO-Y4 apoptosis is p38-dependent- As it seems that TZDs have PPAR-γ independent mechanisms, we thought to determine whether osteocyte apoptosis and sclerostin up-regulation were under PPAR-γ control (Figure 3). In the presence of TZDs, an increase in osteocyte apoptosis was observed. Silencing of PPAR-γ did not modify the pattern of osteocyte apoptosis. These results suggest that TZDs induce osteocyte apoptosis through a PPAR-γ independent mechanism (Figure 3A). On the other hand, sclerostin up-regulation was dramatically decreased by 71% and 54% in pioglitazone- and rosiglitazone-treated cultures respectively in the absence of PPAR-γ (Figure 3B). Furthermore, in the promoter of the murine sclerostin gene we found a putative sequence for PPAR-γ binding in -1832 (data not shown), reinforcing the idea that sclerostin expression might be under the control of PPAR-γ. Rapidly after activation with TZDs, PPAR-γ is phosphorylated on serine 84 (Supplemental Figure S1A). The phosphorylation remained even in the presence of FR180204 and SB203580 (Supplemental Figure S1B). Our next questions were to investigate whether osteocytes apoptosis and sclerostin up-regulation, in response to TZDs, were mediated by activation of Erk1/2 and/or p38 (Figure 4). In the presence of 10µM FR180204, a specific Erk1/2 inhibitor, osteocyte apoptosis was slightly increased by 13% and 10% in pioglitazone- and rosiglitazone-treated cultures respectively (Figure 4A). On the other hand, in the presence of 10µM SB203580, a specific p38 inhibitor, osteocyte apoptosis was significantly decreased by 69% and 63% in pioglitazone- and rosiglitazone-treated cultures, respectively. As Erk1/2 and p38 are known modulator of cell growth, MLO-Y4 cells were

cultured in reduced serum conditions. Arresting cell growth did not affect the pattern of osteocyte death but the presence of SB203580 significantly lowered the amount of dead osteocytes in low serum condition, suggesting that TZDs induce osteocyte death, independently of cell growth, via a p38-dependent mechanism (Supplemental Figure S2). We also looked at sclerostin expression and we found that the presence of FR180204 or SB203580 did not significantly affect the pattern of sclerostin expression in response to TZDs stimulation.

MLO-Y4 apoptosis is mediated through GPR–40- In other cell systems, it has been reported that TZDs activate a cell surface receptor called GPR40. We thought to determine whether osteocytes expressed GPR40. Indeed, by Western blot, we found that GPR40 is abundantly expressed in osteocytes (Figure 5A) but also in human osteoblasts and primary human osteoclasts. Furthermore, immunogold labelling revealed that GPR40, on osteocytes, is localised at the cell membrane (Figure 5B). In order to investigate whether GPR40 could be a target for TZDs in osteocytes, we performed silencing experiments. After 72 hours, GPR40 expression was significantly reduced by 92% (Figure 6A). GPR40 silencing resulted in a decreased activation of Erk1/2 and p38 in pioglitazone- and rosiglitazone-treated cultures although this decrease was more marked for p38 (Figure 6B). Osteocyte apoptosis, in response to pioglitazone and rosiglitazone, was significantly decreased by 66% and 70%, respectively in cells where GPR40 was silenced confirming that this cell surface receptor was responsible for p38 activation and osteocyte apoptosis (Figure 6C). On the other hand, sclerostin expression was unchanged in GPR40-silenced cultures in response to TZDs (Figure 6D). Moreover, we investigated the intracytoplasmic localization of Bax in TZD-treated cells (Figure 6E). TZDs trigger a relocalization of Bax from the cytoplasm to the outer membrane of the mitochondria. Silencing of GPR40 or SB203580 treatment reversed the relocalization of Bax.

Thiazolidinediones induce cell death and sclerostin up-regulation in primary osteoblasts- In order to ascertain whether the above findings were restricted to the MLO-Y4 cell line or could be extended to bone-derived osteoblasts, we investigated p38 activation, cell death and sclerostin expression in response to TZDs in osteoblasts obtained from calvariae of young mice (Figure 7). Rapidly after pioglitazone treatment, p38 is activated in primary osteoblasts (Figure 7A). Interestingly, TZD induced a significant augmentation in cell death in osteoblast cultures by 60% and 72% in pioglitazone and rosiglitazone-treated cultures, respectively (Figure 7B). This increase in cell death is mediated, as for MLO-Y4 cells, through a GPR40-p38 mechanism as evidenced by the reduction in cell death in the presence of siRNA targeting GPR40 or SB203580 (Figures 7B and 7C). On the other hand, PPAR-γ silencing did not affect cell death in TZD-treated cultures (Figure 7D). Similarly to what was observed with MLO-Y4 cells, TZDs significantly up-regulated sclerostin expression. On the other hand, sclerostin expression was not affected by GPR40 silencing (data not shown) but as for MLO-Y4, sclerostin expression was significantly reduced by 84% in cultures where PPAR-γ was silenced.

Thiazolidinediones decreased osteoclast formation through a GPR40/p38-mediated mechanism- As GPR40 was expressed also in osteoclasts, we investigated the role of TZD in osteoclast physiology. In opposition to what was reported for primary osteoblasts and MLO-Y4 cells, TZDs do not raise the death of osteoclast precursors (Figure 8). However, although cell death was not affected, osteoclast precursor cultures treated with TZDs resulted in a dose-dependent decrease in osteoclast numbers. We then postulated that the same GPR40/p38 mechanism might be responsible for this reduction in osteoclast numbers. And indeed, silencing of GPR40 or use of SB203580, significantly increased the number of osteoclast as evidenced in Figure 8C and 8D.

Discussion

Thiazolidinediones represent an interesting class of drugs used in the treatment of type 2 diabetes mellitus. However, several adverse effects including low bone mass and bone fracture have been reported in patients treated with these molecules. Previously, we reported that TZDs induce sclerostin expression and osteocytes apoptosis (17). However, little was known about the molecular mechanism leading to these two events and especially whether they were the

results of distinct molecular pathways or linked. In the present study, our results suggest that although TZDs induce sclerostin expression through activation of PPAR-γ, osteocyte apoptosis is mediated through a different signalling pathway involving GPR40, proteins from the Ras superfamily and activation of Erk 1/2 and p38.

TZDs have previously been described as agonists of PPAR-γ. The ligand binding affinities order for PPAR-γ is rosiglitazone > pioglitazone > troglitazone (27). However, although TZDs mediate osteocyte apoptosis, the ranking order for TZD potency in doing this effect is pioglitazone > troglitazone > rosiglitazone (27). This finding is in contradiction with the ligand binding affinities. In the present study, we reported that silencing of PPAR-γ did not affect the pattern of osteocyte apoptosis whereas silencing of GPR40 significantly decreased osteocyte apoptosis. Furthermore, blockade of p38, which is activated within 15 minutes in osteocytes, kinetically appear unlikely to reflect actions toward PPAR-γ. Taken together, these results indicate that although TZDs have been described as strong PPAR-γ agonists, some effects are mediated through different intracellular signalling pathways. On the other hand, the order of potency regarding sclerostin expression seems to follow the ligand binding affinities and is markedly reduced when PPAR-γ was silenced, suggesting a PPAR-γ-dependent mechanism. This idea is further reinforced by the fact that a putative PPAR-γ responsive element could be identified in the promoter of the Sost gene. The molecular mechanism leading to PPARγ activation by TZDs is still unclear. PPARγ activity may be modulated by several post-translational modifications including phosphorylation, sumoylation, ubiquitination, nitration and intracellular compartimentalization (see review in(28)). Some of our results suggested an increase in serine 84 phosphorylation in response to TZDs, however this phosphorylation seemed to be independent of Erk 1/2 and p38 activation as specific inhibitors such as FR180204 and SB203580 did not modify the pattern of serine 84 phosphorylation. Further studies are clearly required to fully understand the mechanism behind PPARγ activation and sclerostin up-regulation.

Although TZDs signal with no doubt through PPAR-γ, several other signalling pathways have been evidenced (18,29-34). Among all of these pathways, similarities in intracellular targets have been evidenced with transactivation of the epidermal growth factor receptor. As such, in liver cells, transactivation of this receptor (30,32,33) leads to activation of Erk and p38. This pathway involved the rapid generation of reactive oxygen species to activate src and then EGFR. However, in our study, we demonstrated that in osteocytes, TZDs did not generate an oxidative stress and it is unlikely that this pathway is at the origin of osteocyte apoptosis. A strong argument to emphasise the role of GPR40 in osteocyte apoptosis is that MAP Kinase signalling and osteocyte apoptosis were strongly inhibited in the presence of GPR40 silencing. Furthermore, several recent studies reported the involvement of GPR40 in PPAR-γ independent response to TZDs in other cell types (35,36). Smith et al., reported recently the mode of binding of TZDs to GPR40 and demonstrated that upon binding, a rapid activation of $G\alpha_q/G\alpha_{11}$ resulting in activation of Erk 1/2 and p38 (18). Our study suggests similar results as TZDs induce Erk 1/2 and p38 activation upon interaction with GPR40. Our study also seems suggest that Ras proteins are intermediates between GPR40 and MAP kinase activation. However, whether this event requires $G\alpha_q/G\alpha_{11}$ and increase intracellular calcium concentration remains unknown.

According to our knowledge, we reported for the first time in the present study the expression of GPR40, the free fatty acid receptor 1, at the surface of osteocytes. Cornish et al., previously reported the expression of GPR40 in murine osteoclast precursor cells but not in murine osteoblasts (37). Cornish et al reported that the use of GW9508, a GPR40/GPR120 agonist, resulted in decreased osteoclastogenesis. Our results in osteoclast cultures support also a role of GPR40 in reducing osteoclastogenesis. Recently, a growing body of evidence suggested that PPAR-γ is necessary for osteoclastogenesis (38,39), however, this is intriguing as TZDs have been shown to decrease osteoclast formation and bone resorption (40-42). One explanation could be that in osteoclasts, the

observed effect associated with the use of TZDs is mediated through GPR40 and as such further studies on the impact of GPR40 activation in osteoclasts are needed.

As a conclusion, Figure 9 summarises the effects of TZDs on osteocytes. Rapidly after treatment with TZDs, phosphorylation of Erk 1/2 and p38 occurs through the involvement of GPR40, expressed at the cytoplasmic membrane and Ras. This signalling pathway results in recruitment of Bax at the outer membrane of the mitochondria and induction of osteocytes apoptosis. In parallel, TZDs crossed the cytoplasmic membrane and activate PPAR-γ. In return PPAR-γ induces the expression within 24 hours of sclerostin.

Acknowledgments

This work was made possible by grants from Contrat Région Pays de la Loire: Bioregos2 program.

References

1. Kawai, M., and Rosen, C. J. (2010) *Nat Rev Endocrinol* **6**, 629-636
2. Kahn, S. E., Haffner, S. M., Heise, M. A., Herman, W. H., Holman, R. R., Jones, N. P., Kravitz, B. G., Lachin, J. M., O'Neill, M. C., Zinman, B., and Viberti, G. (2006) *N Engl J Med* **355**, 2427-2443
3. Dormandy, J. A., Charbonnel, B., Eckland, D. J., Erdmann, E., Massi-Benedetti, M., Moules, I. K., Skene, A. M., Tan, M. H., Lefebvre, P. J., Murray, G. D., Standl, E., Wilcox, R. G., Wilhelmsen, L., Betteridge, J., Birkeland, K., Golay, A., Heine, R. J., Koranyi, L., Laakso, M., Mokan, M., Norkus, A., Pirags, V., Podar, T., Scheen, A., Scherbaum, W., Schernthaner, G., Schmitz, O., Skrha, J., Smith, U., and Taton, J. (2005) *Lancet* **366**, 1279-1289
4. Kahn, S. E., Zinman, B., Lachin, J. M., Haffner, S. M., Herman, W. H., Holman, R. R., Kravitz, B. G., Yu, D., Heise, M. A., Aftring, R. P., and Viberti, G. (2008) *Diabetes Care* **31**, 845-851
5. Meymeh, R. H., and Wooltorton, E. (2005) *CMAJ* **177**, 723-724
6. Lecka-Czernik, B., Gubrij, I., Moerman, E. J., Kajkenova, O., Lipschitz, D. A., Manolagas, S. C., and Jilka, R. L. (1999) *J Cell Biochem* **74**, 357-371
7. Lecka-Czernik, B., Moerman, E. J., Grant, D. F., Lehmann, J. M., Manolagas, S. C., and Jilka, R. L. (2002) *Endocrinology* **143**, 2376-2384
8. Berberoglu, Z., Gursoy, A., Bayraktar, N., Yazici, A. C., Bascil Tutuncu, N., and Guvener Demirag, N. (2007) *J Clin Endocrinol Metab* **92**, 3523-3530
9. Glintborg, D., Andersen, M., Hagen, C., Heickendorff, L., and Hermann, A. P. (2008) *J Clin Endocrinol Metab* **93**, 1696-1701
10. Grey, A., Bolland, M., Gamble, G., Wattie, D., Horne, A., Davidson, J., and Reid, I. R. (2007) *J Clin Endocrinol Metab* **92**, 1305-1310
11. Jennermann, C., Triantafillou, J., Cowan, D., Pennink, B., Connolly, K., and Morris, D. (1995) *J Bone Miner Res* **10**, S241
12. Rzonca, S. O., Suva, L. J., Gaddy, D., Montague, D. C., and Lecka-Czernik, B. (2004) *Endocrinology* **145**, 401-406
13. Bonewald, L. F. (2008) Osteocytes. in *Primer on the metabolic bone diseases and disorders of mineral metabolism* (Rosen, C. J. ed.), 7th Ed., American Society for Bone and Mineral Research, Washington D.C. pp 22-27
14. Plotkin, L. I., Aguirre, J. I., Kousteni, S., Manolagas, S. C., and Bellido, T. (2005) *J Biol Chem* **280**, 7317-7325
15. Plotkin, L. I., Lezcano, V., Thostenson, J., Weinstein, R. S., Manolagas, S. C., and Bellido, T. (2008) *J Bone Miner Res* **23**, 1712-1721
16. Zhao, S., Zhang, Y. K., Harris, S., Ahuja, S. S., and Bonewald, L. F. (2002) *J Bone Miner Res* **17**, 2068-2079
17. Mabilleau, G., Mieczkowska, A., and Edmonds, M. E. (2010) *Diabet Med* **27**, 925-932
18. Smith, N. J., Stoddart, L. A., Devine, N. M., Jenkins, L., and Milligan, G. (2009) *J Biol Chem* **284**, 17527-17539

19. Stoddart, L. A., Brown, A. J., and Milligan, G. (2007) *Mol Pharmacol* **71**, 994-1005
20. Alquier, T., Peyot, M. L., Latour, M. G., Kebede, M., Sorensen, C. M., Gesta, S., Ronald Kahn, C., Smith, R. D., Jetton, T. L., Metz, T. O., Prentki, M., and Poitout, V. (2009) *Diabetes* **58**, 2607-2615
21. Latour, M. G., Alquier, T., Oseid, E., Tremblay, C., Jetton, T. L., Luo, J., Lin, D. C., and Poitout, V. (2007) *Diabetes* **56**, 1087-1094
22. Kato, Y., Windle, J. J., Koop, B. A., Mundy, G. R., and Bonewald, L. F. (1997) *J Bone Miner Res* **12**, 2014-2023
23. Dumas, A., Gaudin-Audrain, C., Mabilleau, G., Massin, P., Hubert, L., Basle, M. F., and Chappard, D. (2006) *Biomaterials* **27**, 4204-4211
24. Takahashi, N., Udagawa, N., Tanaka, S., and Suda, T. (2003) *Methods Mol Med* **80**, 129-144
25. Mabilleau, G., Chappard, D., and Sabokbar, A. (2011) *J Biol Chem* **286**, 3242-3249
26. Mabilleau, G., Moreau, M. F., Filmon, R., Basle, M. F., and Chappard, D. (2004) *Biomaterials* **25**, 5155-5162
27. Mabilleau, G., Chappard, D., and Basle, M. F. (2011) *Int J Biochem Mol Biol* **2**, 240-246
28. Luconi, M., Cantini, G., and Serio, M. (2010) *Steroids* **75**, 585-594
29. Colca, J. R., McDonald, W. G., Waldon, D. J., Leone, J. W., Lull, J. M., Bannow, C. A., Lund, E. T., and Mathews, W. R. (2004) *Am J Physiol Endocrinol Metab* **286**, E252-260
30. Dewar, B. J., Gardner, O. S., Chen, C. S., Earp, H. S., Samet, J. M., and Graves, L. M. (2007) *Mol Pharmacol* **72**, 1146-1156
31. Fryer, L. G., Parbu-Patel, A., and Carling, D. (2002) *J Biol Chem* **277**, 25226-25232
32. Gardner, O. S., Dewar, B. J., Earp, H. S., Samet, J. M., and Graves, L. M. (2003) *J Biol Chem* **278**, 46261-46269
33. Gardner, O. S., Dewar, B. J., and Graves, L. M. (2005) *Mol Pharmacol* **68**, 933-941
34. Takeda, K., Ichiki, T., Tokunou, T., Iino, N., and Takeshita, A. (2001) *J Biol Chem* **276**, 48950-48955
35. Gras, D., Chanez, P., Urbach, V., Vachier, I., Godard, P., and Bonnans, C. (2009) *Am J Physiol Lung Cell Mol Physiol* **296**, L970-978
36. Wu, P., Yang, L., and Shen, X. (2010) *Biochem Biophys Res Commun* **403**, 36-39
37. Cornish, J., MacGibbon, A., Lin, J. M., Watson, M., Callon, K. E., Tong, P. C., Dunford, J. E., van der Does, Y., Williams, G. A., Grey, A. B., Naot, D., and Reid, I. R. (2008) *Endocrinology* **149**, 5688-5695
38. Wan, Y., Chong, L. W., and Evans, R. M. (2007) *Nat Med* **13**, 1496-1503
39. Wei, W., Wang, X., Yang, M., Smith, L. C., Dechow, P. C., Sonoda, J., Evans, R. M., and Wan, Y. (2010) *Cell Metab* **11**, 503-516
40. Chan, B. Y., Gartland, A., Wilson, P. J., Buckley, K. A., Dillon, J. P., Fraser, W. D., and Gallagher, J. A. (2007) *Bone* **40**, 149-159
41. Mbalaviele, G., Abu-Amer, Y., Meng, A., Jaiswal, R., Beck, S., Pittenger, M. F., Thiede, M. A., and Marshak, D. R. (2000) *J Biol Chem* **275**, 14388-14393
42. Okazaki, R., Toriumi, M., Fukumoto, S., Miyamoto, M., Fujita, T., Tanaka, K., and Takeuchi, Y. (1999) *Endocrinology* **140**, 5060-5065

Footnotes

The abbreviations used are: TZDs, thiazolidinediones; PIO, pioglitazone; ROSI, rosiglitazone; PPAR-γ, peroxisome proliferator-activated receptor-gamma, GPR40, G protein coupled receptor-40

Figure Legends

Figure 1: Pioglitazone (PIO), rosiglitazone (ROSI) and troglitazone (TRO) induce Erk 1/2 and p38 phosphorylation via a PPAR-γ independent mechanism. (A) TZDs at a concentration of 10^{-6}M

induced a rapid activation of Erk 1/2 and p38 in MLO-Y4 cells. Black bars represent pioglitazone, white bars, rosiglitazone and grey bars, troglitazone (B) Erk 1/2 and p38 activation were investigated in siRNA-treated cultures. Silencing of PPAR-γ did not affect the pattern of Erk 1/2 and p38 activation. (C) MLO-Y4 cells treated with phorbol myristate acetate (PMA) significantly increased the production of reactive oxygen species whilst TZDs failed to induce such response. **: $p<0.01$ vs. control cultures.

Figure 2: Ras but not PKC is required for Erk 1/2 and p38 activation in TZDs-treated cultures. Bisindoleimide I (A), a specific inhibitor of PKC, and farnesylthiosalicylic acid (B), a specific inhibitor of ras were used in the culture prior to addition of 10^{-6}M pioglitazone (PIO) or rosiglitazone (ROSI). Phosphorylation of Erk 1/2 and p38 was assessed after 0, 15, 30 and 60 minutes. **: $p<0.01$ vs. untreated cells.

Figure 3: Sclerostin expression but not osteocyte apoptosis is mediated through PPAR-γ. (A) MLO-Y4 cells were pretreated with scrambled (white bars) or ppar-γ siRNA (grey bars) prior to addition of TZDs and osteocytes apoptosis was investigated. Untreated cells (black bars) served as controls. (B) Sclerostin expression was assessed in untreated cells (- or black bars), cells transfected with scrambled siRNA (sc or white bars) and cells transfected with ppar-γ siRNA (ppar-γ or grey bars). **: $p<0.01$ vs. cells transfected with scrambled siRNA.

Figure 4: Osteocyte apoptosis but not sclerostin expression is dependent of Erk 1/2 and p38 activation. (A) MLO-Y4 cells were pretreated with 10 µM FR180204 (white bars), a specific inhibitor of Erk 1/2 or 10 µM SB203580 (grey bars), a specific inhibitor of p38, prior to the addition of 10^{-6}M TZDs in the culture. Black bars represent untreated cells and served as controls. (B) Sclerostin expression was assessed in untreated cells (black bars), FR180204-treated cells (FR or white bars) and in SB203580-treated cells (SB or grey bars). **: $p<0.01$ vs. untreated cells.

Figure 5: GPR40 is expressed at the surface of osteocytes. (A) Detection of GPR40 by Western blot in protein extracts of human osteoblasts (Ob), murine osteocytes (Ocy) and human primary osteoclasts (Oc). (B) Immunogold labelling of GPR40 revealed its presence only at the cytoplasmic membrane (b). GPR40 is not found neither at the nuclear membrane (c), Golgi apparatus (d), mitochondria (e) nor rough endoplasmic reticulum (f). Arrow indicates the localisation of gold beads.

Figure 6: Osteocyte apoptosis but not sclerostin expression is GPR40-dependent. (A) Efficiency of GPR40 silencing, (B) silencing of GPR40 resulted in decrease activation of Erk 1/2 and p38. White bars represent cells transfected with scrambled siRNA and grey bars cells transfected with GPR40 siRNA. (C) Osteocyte apoptosis was determined in response to TZDs in untreated cells (black bars), cells transfected with scrambled siRNA (white bars) and cells transfected with GPR40 siRNA (grey bars). (D) GPR40 silencing did not affect the pattern of expression of sclerostin. White bars represent cells transfected with scrambled siRNA and grey bars cells transfected with GPR40 siRNA. **: $p<0.01$ vs. cells transfected with scrambled siRNA. (E) Intracytoplasmic localization of Bax in untreated cells (a), pioglitazone-treated cells (b), rosiglitazone-treated cells (c), pioglitazone-treated cells transfected with scrambled siRNA (d), pioglitazone-treated cells transfected with GPR40 siRNA and pioglitazone- and SB203580-treated cells (f).

Figure 7: TZDs treatment result also in primary osteoblast death and sclerostin up-regulation. (A) p38 was activated rapidly after pioglitazone treatment in primary osteoblasts. (B) Cell death was assessed in primary osteoblasts cultured with 10^{-6}M TZDs (black bars). Cell death was also determined in osteoblast cultures transfected with either a scrambled siRNA (white bars) or GPR40 siRNA (grey bars). **: $p<0.01$ vs. untreated cells, ##: $p<0.01$ vs scrambled siRNA. (C) Cell death mediated by TZDs was abolished in cells pre-treated with SB203580. **: $p<0.01$ vs. non pre-treated cells. (D) Silencing of PPAR-γ did not affect cell death. (E) Sclerostin expression was significantly augmented in pioglitazone-treated cells but reduced in the absence of PPAR-γ in pioglitazone-treated cells. ##: $p<0.01$ vs scrambled siRNA.

Figure 8: TZDs modulates osteoclastogenesis through a GPR40/p38-dependent mechanism. (A) Bone marrow macrophages were cultured in presence of TZDs for 24hrs prior to cell death assessment. (B) Bone marrow macrophages were cultured in the presence of 25ng/ml M-CSF, 100 ng/ml RANKL and various concentration of pioglitazone prior to osteoclast counting. **: $p<0.01$ vs. previous pioglitazone concentration. (C) GPR40 silencing restored osteoclastogenesis. Bone marrow macrophages were pretreated with either scrambled siRNA (white bars) or GPR40 siRNA (grey bars) prior to the addition of 10^{-6}M TZDs in the culture. **: $p<0.01$ vs. cells transfected with scrambled siRNA. (D) Inhibition of p38 restored osteoclastogenesis. Bone marrow macrophages were pretreated with 10 µM SB203580 (grey bars) prior to the addition of 10^{-6}M TZDs in the culture. Black bars represent untreated cells and served as controls. **: $p<0.01$ vs. cells not treated with SB203580.

Figure 9: Schematic representation of TZDs action in osteocytes. TZDs activate two distinct signalling pathways: first, TZDs bind GPR40 and rapidly activate Erk 1/2 and p38 through a ras-dependent mechanism. This pathway leads to recruitment of BAX at the outer membrane of the mitochondria and osteocyte apoptosis. TZDs also bind to PPAR-γ and this results in activation of the sclerostin gene (SOST) and sclerostin up-regulation.

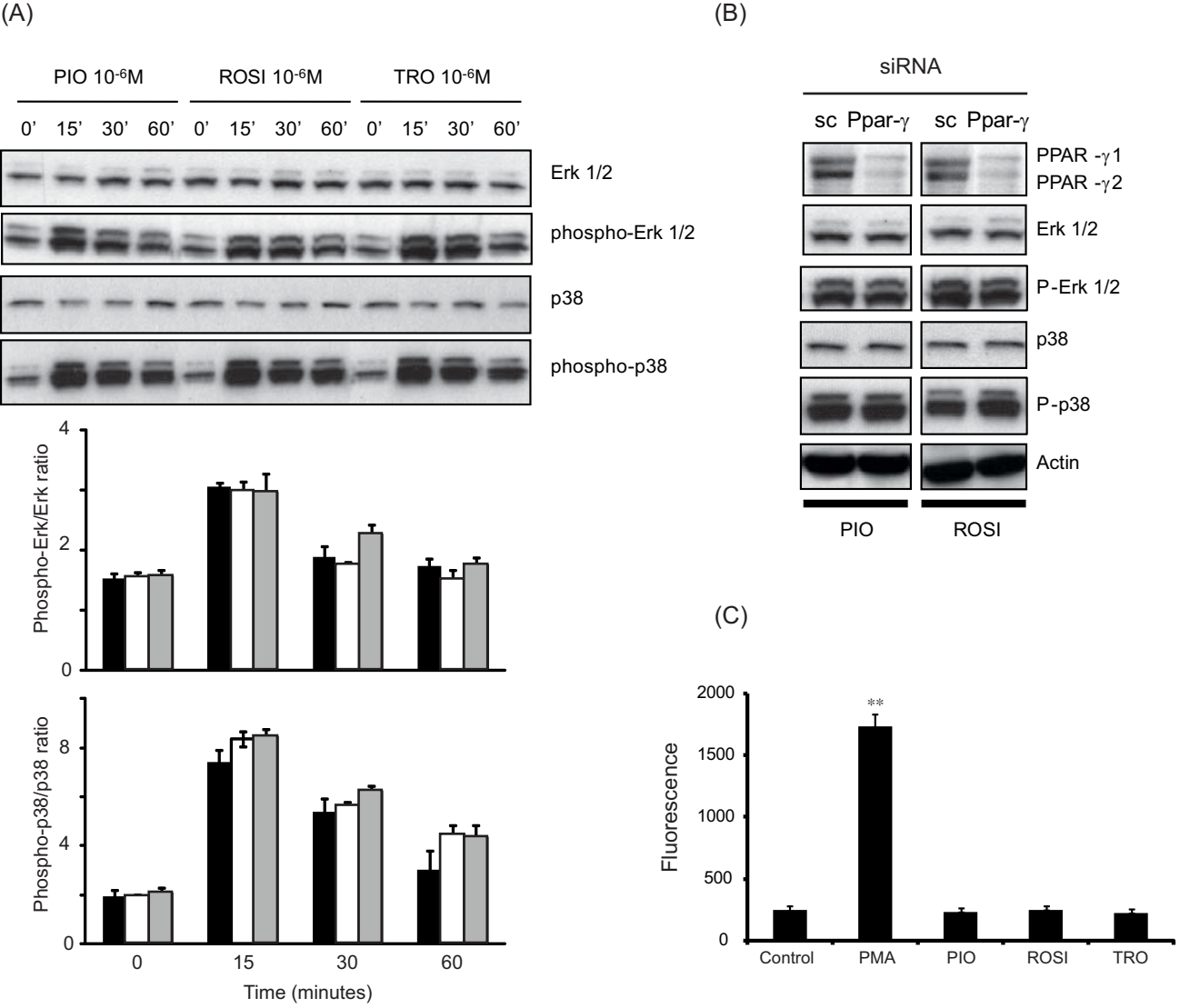
(A)
PIO 10-6M
ROSI 10-6M
TRO 10-6M
0' 15' 30' 60' 0' 15' 30' 60' 0' 15' 30' 60'
Erk 1/2
phospho-Erk 1/2
p38
phospho-p38
Phospho-Erk/Erk ratio
Phospho-p38/p38 ratio
Time (minutes)
(B)
siRNA
sc Ppar-γ sc Ppar-γ
PPAR -γ1
PPAR -γ2
Erk 1/2
P-Erk 1/2
p38
P-p38
Actin
PIO
ROSI
(C)
Fluorescence
Control
PMA
PIO
ROSI
TRO

Figure 1

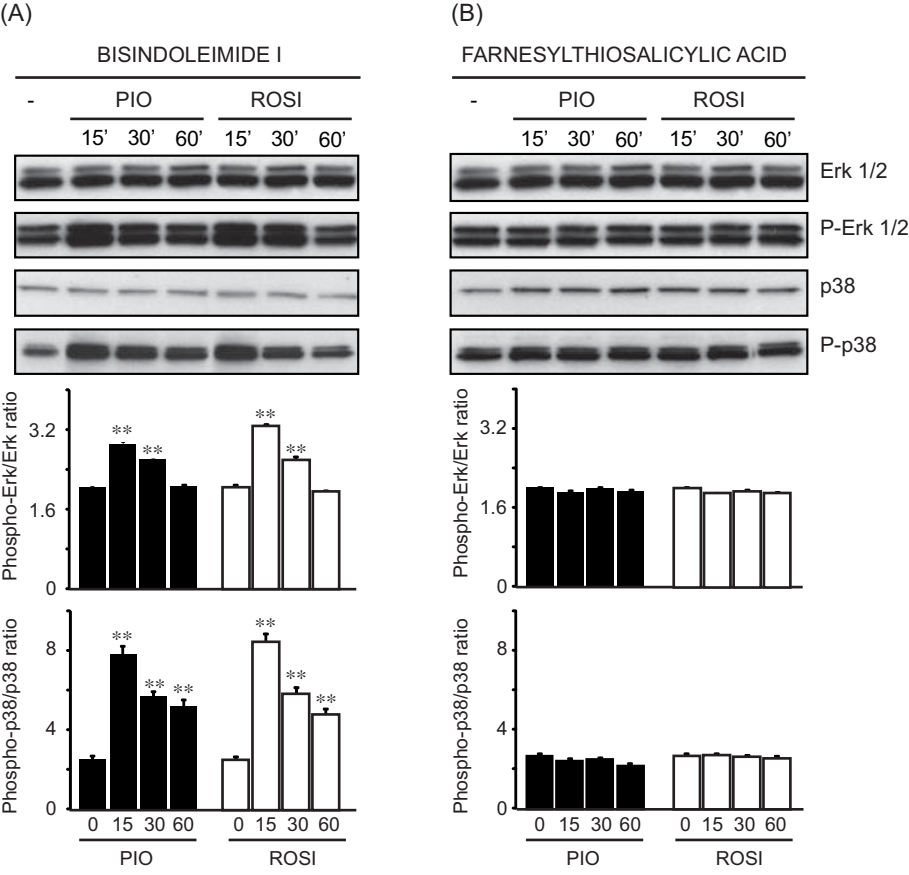
(A)
BISINDOLEIMIDE I
-
PIO
ROSI
15' 30' 60' 15' 30' 60'
Phospho-Erk/Erk ratio
3.2
1.6
0
Phospho-p38/p38 ratio
8
4
0
0 15 30 60 0 15 30 60
PIO
ROSI
(B)
FARNESYLTHIOSALICYLIC ACID
-
PIO
ROSI
15' 30' 60' 15' 30' 60'
Erk 1/2
P-Erk 1/2
p38
P-p38
Phospho-Erk/Erk ratio
3.2
1.6
0
Phospho-p38/p38 ratio
8
4
0
0 15 30 60 0 15 30 60
PIO
ROSI

FIGURE 2

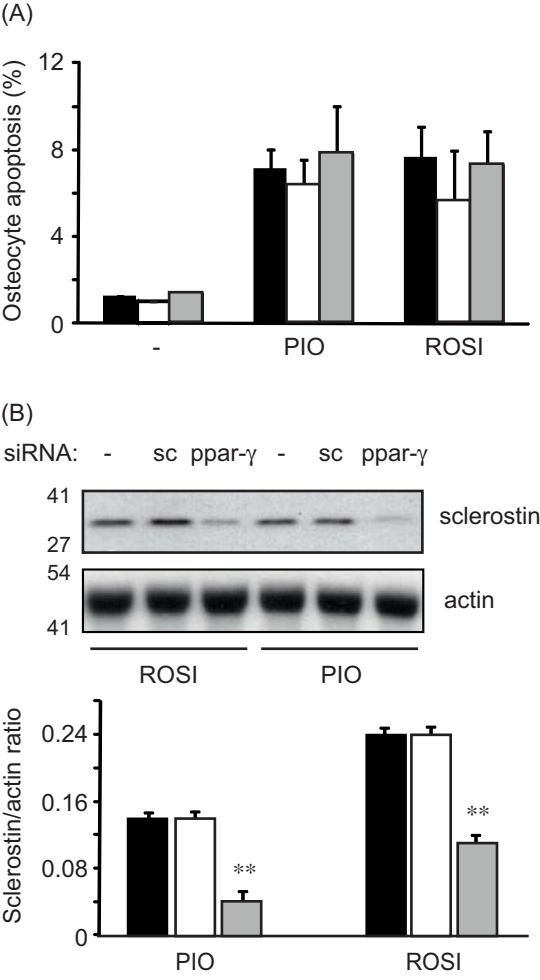
(A)
Osteocyte apoptosis (%)
12
8
4
0
-
PIO
ROSI
(B)
siRNA: - sc ppar-γ - sc ppar-γ
41
27
sclerostin
54
41
actin
ROSI
PIO
Sclerostin/actin ratio
0.24
0.16
0.08
0
**
**
PIO
ROSI

FIGURE 3

(A)

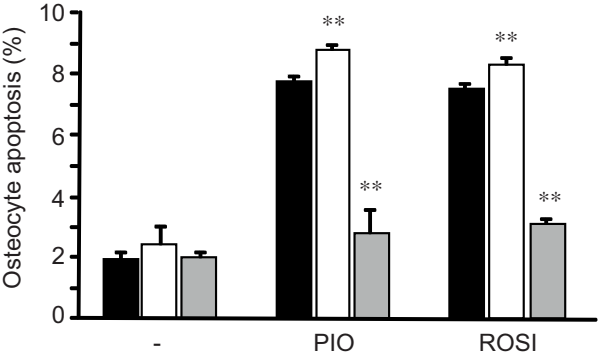
Osteocyte apoptosis (%)
10
8
6
4
2
0
**
**
**
**
-
PIO
ROSI

(B)

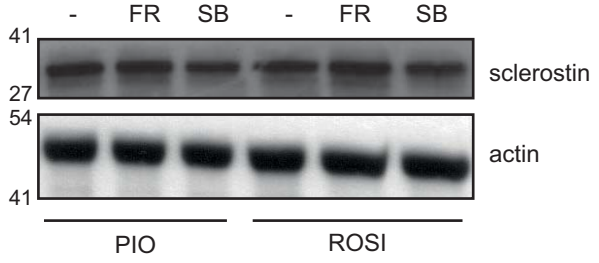
-
FR
SB
-
FR
SB
41
27
54
41
sclerostin
actin
PIO
ROSI

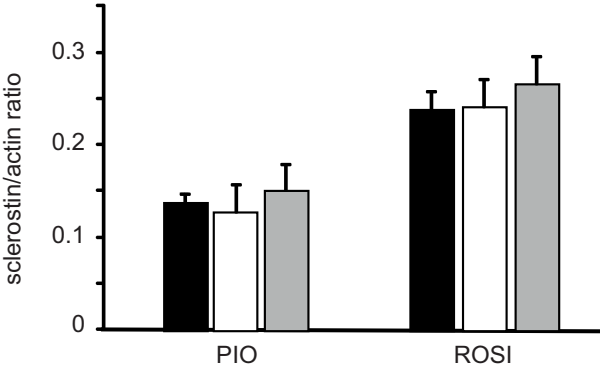
sclerostin/actin ratio
0.3
0.2
0.1
0
PIO
ROSI

FIGURE 4

(A)

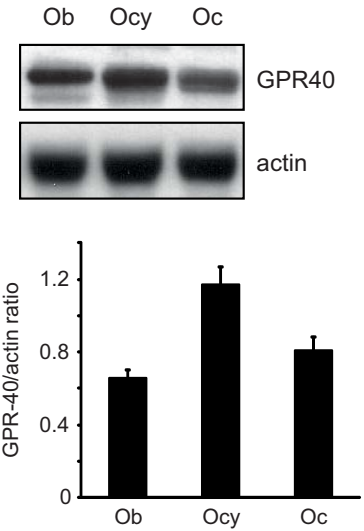
Ob
Ocy
Oc
GPR40
actin
GPR-40/actin ratio
1.2
0.8
0.4
0
Ob
Ocy
Oc

(B)

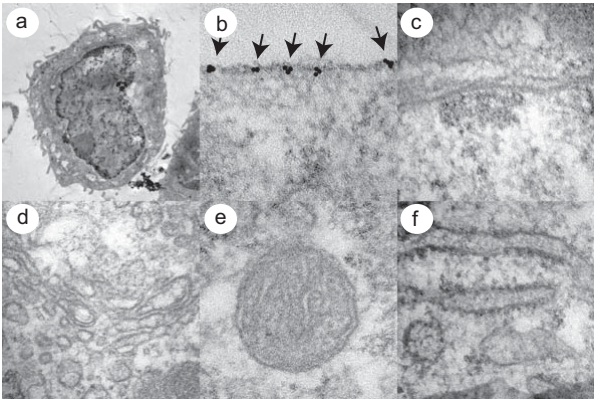
a
b
c
d
e
f

Figure 5

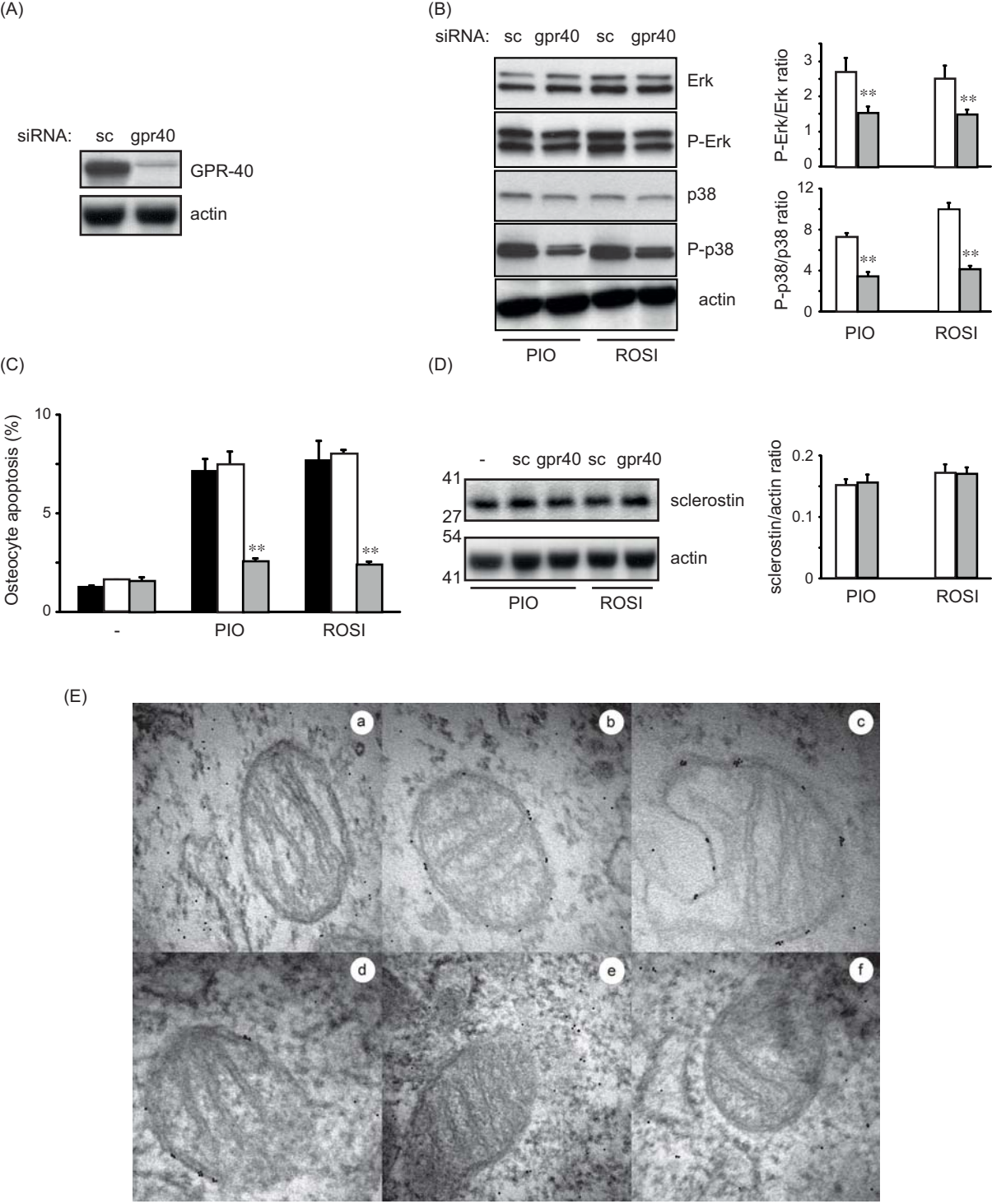
(A)
siRNA: sc gpr40
GPR-40
actin
(B)
siRNA: sc gpr40 sc gpr40
Erk
P-Erk
p38
P-p38
actin
PIO
ROSI
P-Erk/Erk ratio
P-p38/p38 ratio
**
(C)
Osteocyte apoptosis (%)
-
PIO
ROSI
(D)
- sc gpr40 sc gpr40
41
27
54
41
sclerostin
actin
PIO
ROSI
sclerostin/actin ratio
(E)
a
b
c
d
e
f

Figure 6

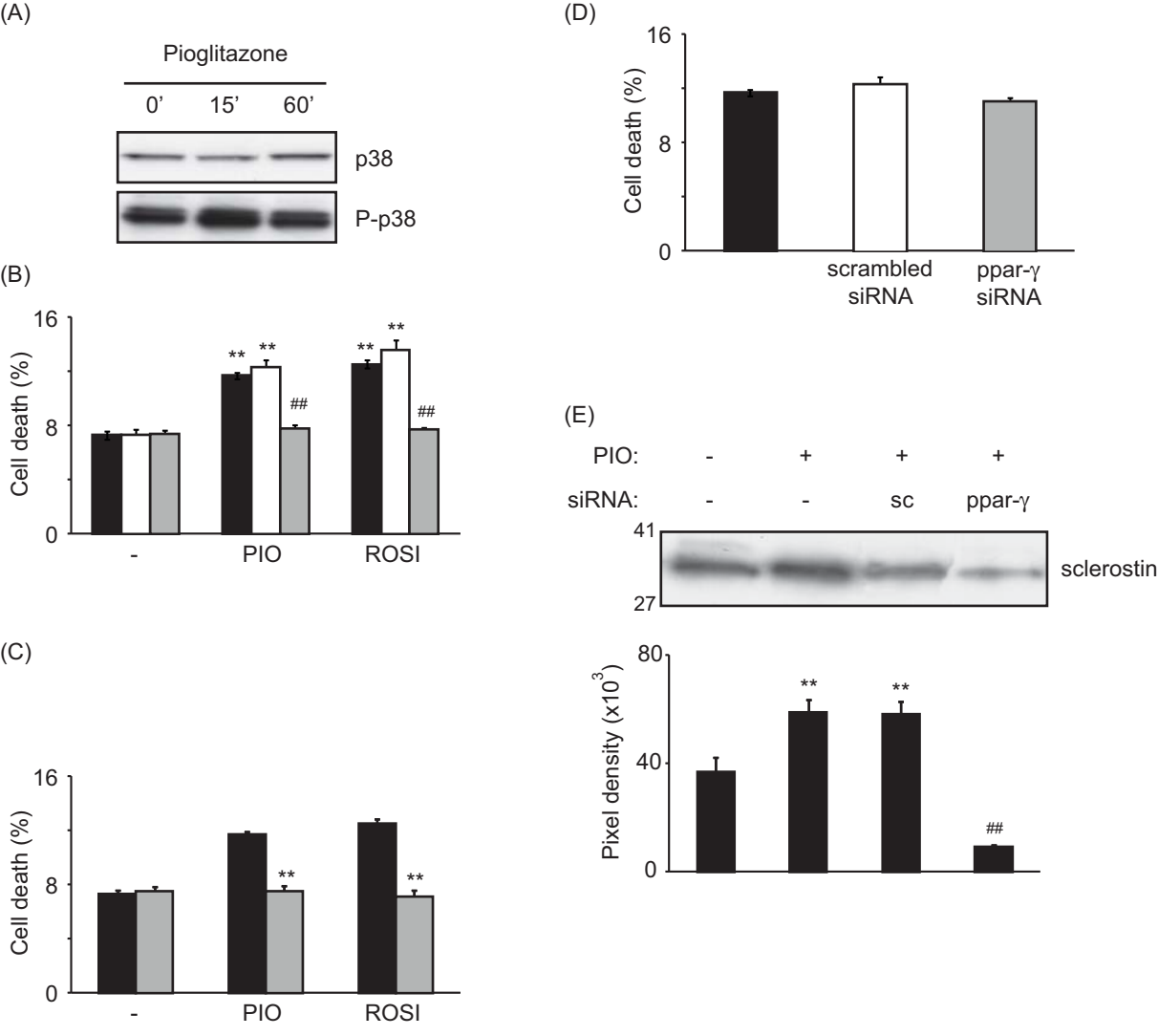
(A)
Pioglitazone
0'
15'
60'
p38
P-p38
(B)
Cell death (%)
16
8
0
**
**
##
**
**
##
-
PIO
ROSI
(C)
Cell death (%)
16
8
0
**
**
-
PIO
ROSI
(D)
Cell death (%)
16
8
0
scrambled siRNA
ppar-γ siRNA
(E)
PIO:
-
+
+
+
siRNA:
-
-
sc
ppar-γ
41
27
sclerostin
Pixel density (x10^3)
80
40
0
**
**
##

FIGURE 7

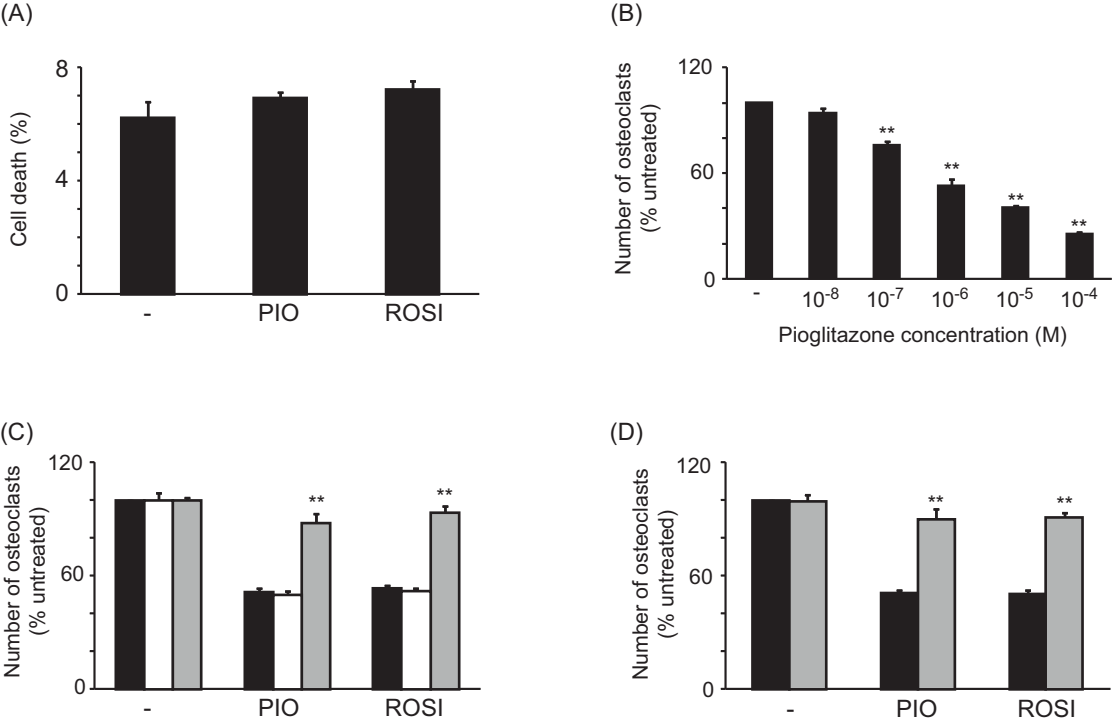
(A)
Cell death (%)
8
4
0
-
PIO
ROSI
(B)
Number of osteoclasts
(% untreated)
120
60
0
**
-
10-8
10-7
10-6
10-5
10-4
Pioglitazone concentration (M)
(C)
Number of osteoclasts
(% untreated)
120
60
0
**
-
PIO
ROSI
(D)
Number of osteoclasts
(% untreated)
120
60
0
**
-
PIO
ROSI

Figure 8

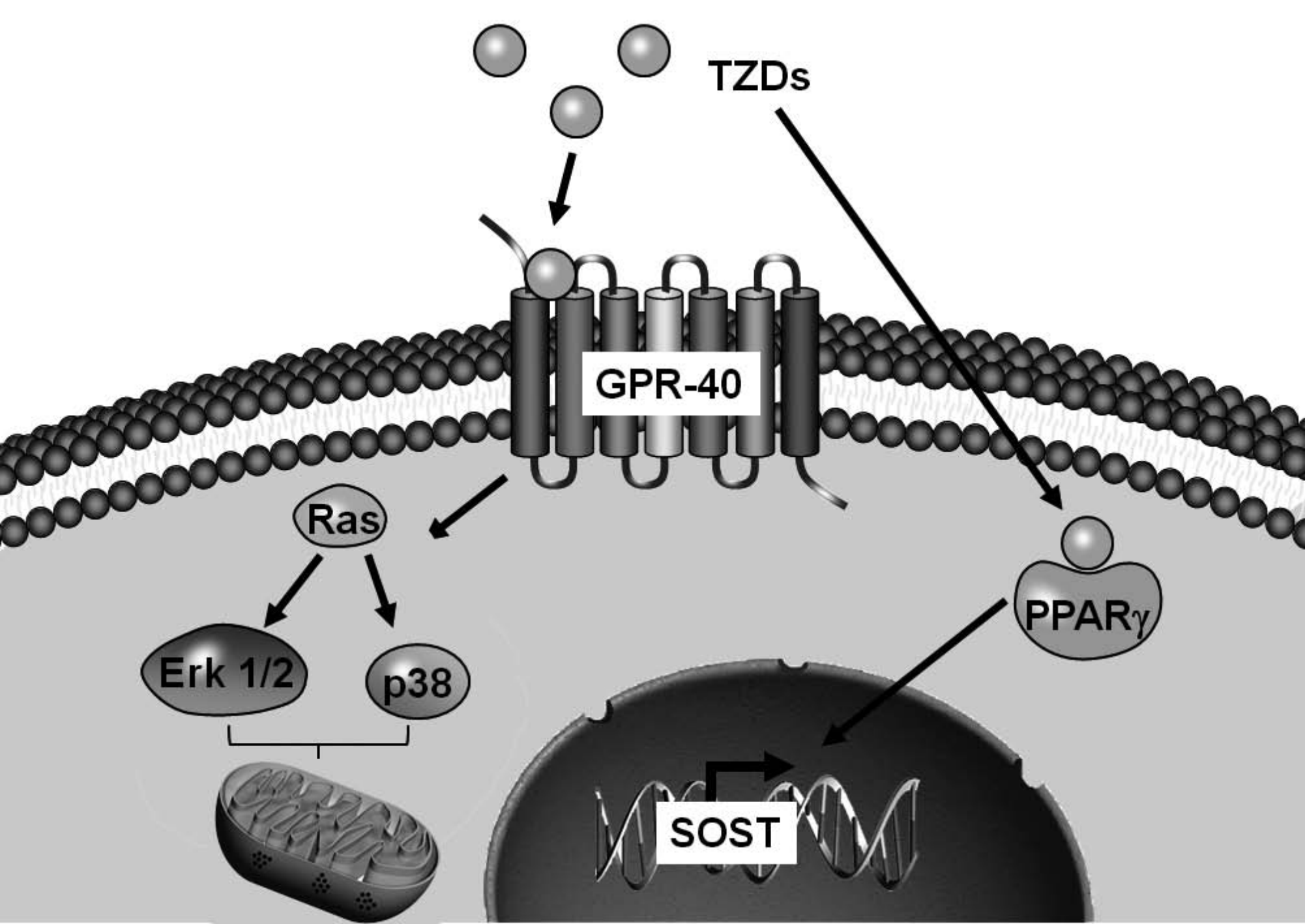
TZDs
GPR-40
Ras
Erk 1/2
p38
PPARγ
SOST

Supplemental figure legends

Supplemental figure S1: PPAR-γ phosphorylation on Ser84 is independent of Erk1/2 and p38 pathways. (A) Rapidly after activation with pioglitazone (PIO), PPAR-γ is phosphorylated on Ser84. (B) Ser84 phosphorylation is not hampered by the use of either FR180204 (FR) or SB203580 (SB).

Supplemental figure S2: Growth arresting MLO-Y4 did not modify the pattern of cell death. (A) By reducing the serum concentration from 10% (dark circles) to 1% (white circles), cell growth was dramatically reduced. (B) Cell death in response to pioglitazone (PIO) or rosiglitazone (ROSI) was not affected by growth arrest. Black bars represent cells cultured in 10% serum and white bars represent cells grown in 1% serum. (C) In reduced serum condition, pioglitazone mediated cell death through a GPR40/p38 mechanism. **: $p<0.01$ vs. pioglitazone alone treatment.

Supplemental Figure S1

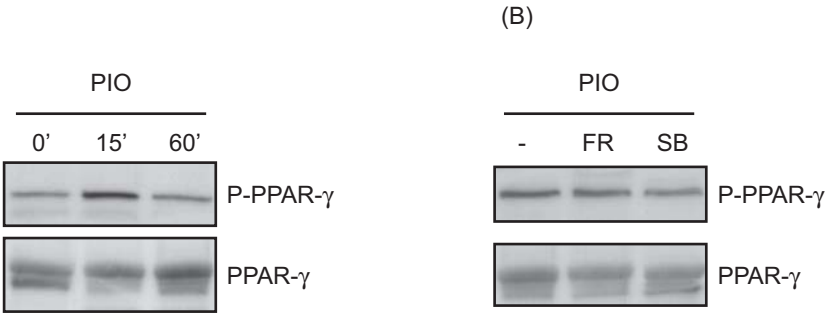
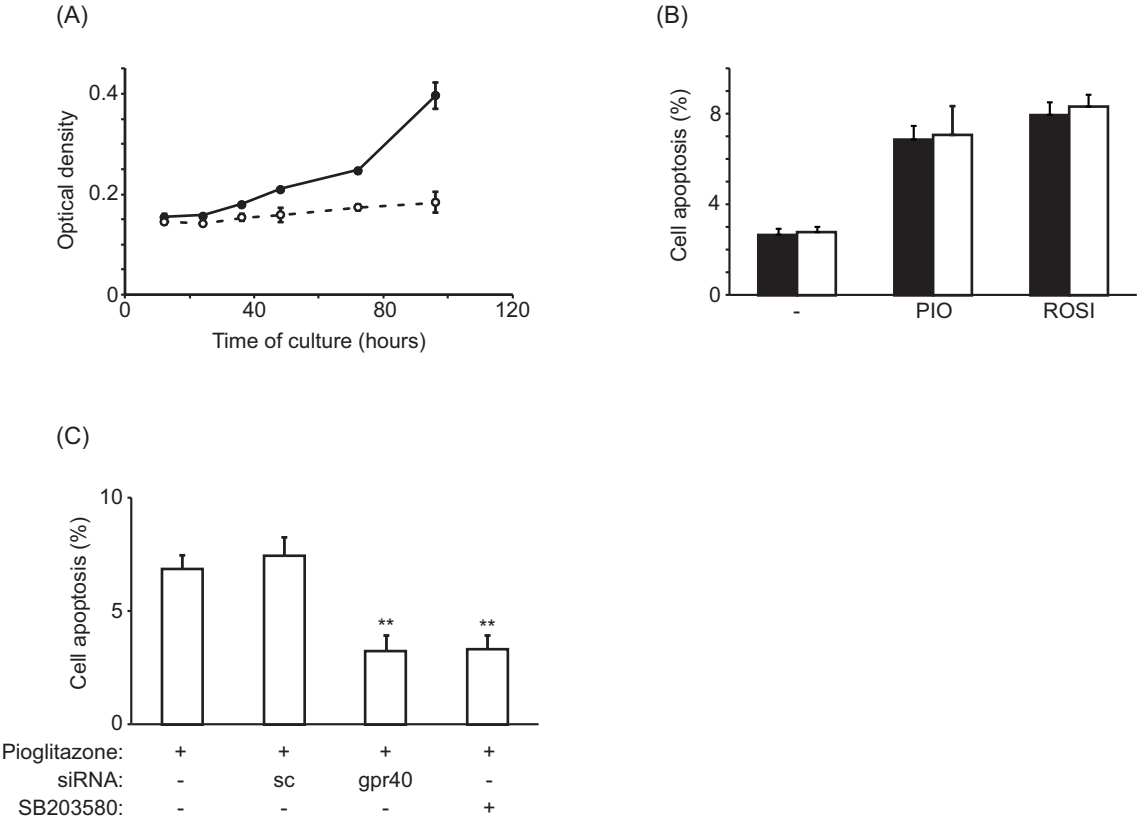
Supplemental Figure S2